Ferromagnetic resonance method for determining the magnetic surface anisotropy of amorphous films

Lu Zhang and George T. Rado
Department of Physics and Astronomy, The Johns Hopkins University, Baltimore, Maryland 21218
(Received 15 December 1986; revised manuscript received 13 July 1987)

The theory of a ferromagnetic resonance (FMR) method for determining the magnetic surface anisotropy of amorphous films is presented. This method enables one to deduce the surface anisotropy constant K_s of an amorphous material from the dependence of the magnetic resonance field on the film thickness. The analysis includes spin-wave modes and surface-induced modes, perpendicular and parallel FMR configurations, and thin as well as ultrathin films. No approximations are made other than the linearization of the equation of motion and the assumption that skin-depth effects and electromagnetic propagation effects are negligible. Good agreement is found between the theory of the method and experimental FMR data on ultrathin films of amorphous Fe-B alloys. The reliability of the K_s values deduced by means of the theory from experimental FMR and superconducting quantum-interference device data is briefly discussed.

I. INTRODUCTION

In a recent paper[1] we reported on ferromagnetic resonance (FMR) measurements of the magnetic surface anisotropy energy of amorphous films. The method used in interpreting the measurements includes an adaptation to amorphous materials of a theory[2] which treats the effects of surface anisotropy on the FMR in ultrathin monocrystalline films. This adaptation makes it possible to deduce the surface anisotropy constant K_s of an amorphous material from the dependence of the magnetic resonance field $H_{\rm res}$ on the film thickness $2L$.

The main purpose of the present paper is to derive and discuss the theory of our FMR method for determining the surface anisotropy of amorphous films. Since Ref. 1 was subject to the length restrictions of a conference paper, its treatment of the theory was confined to a mere listing of the final equations for $H_{\rm res}$. Although the theory for amorphous media is somewhat analogous to that developed for monocrystals,[2] we believe that it is worth presenting the former for its own interest and for the purpose of treating several subjects omitted in the latter. These subjects include (a) spin-wave modes rather than just surface-induced modes, (b) perpendicular rather than just parallel FMR configurations, and (c) thin rather than just ultrathin ferromagnetic films. Our formulation of the theory is, moreover, relatively compact and unified but nevertheless suitable for further extensions.

Also included in the present paper is a more extensive comparison of theory and experiment than was possible in Ref. 1. In particular, we are now in a position to analyze the reliability of the FMR method for measuring K_s. This analysis makes use of our recently obtained experimental magnetization data based on a superconducting quantum-interference device (SQUID) experiment on the alloys used in the FMR experiments.

As to previous work, we note that the literature contains several theoretical and experimental investigations of surface anisotropy and that these have been reviewed by Puszkarski[3] and by Gradmann.[4] In the present paper we report a different method for experimentally determining K_s in amorphous films. Because of the two features discussed below, we believe that this method is more reliable than previous methods. Firstly, we use several values of the film thickness $2L$ for any given material. This means that if we obtain from measurements of $H_{\rm res}$ the same value of K_s for several values of $2L$, as we do in this paper, then our deduced K_s is independent of $2L$ and thus represents a true surface property of the material under investigation. Secondly, we show in this paper that both the FMR data and the SQUID data indicate the magnetization to be homogeneous. Our deduced K_s value represents, therefore, a true surface anisotropy rather than a simulated surface anisotropy caused by an inhomogeneous volume magnetization. We believe that in some previous methods it is the absence of these two features which has led to questionable K_s measurements.

II. THEORY

A. Magnetization equations and boundary conditions

The calculations which follow are based on the equation of motion[5] of the magnetization

$$(1/\gamma)(\partial\mathbf{u}/\partial t)=\mathbf{u}\times[-(1/M)\nabla_u E_v+(2A/M)\nabla^2\mathbf{u}] \quad (1)$$

and on the general exchange boundary condition[6]

$$\mathbf{u}\times[\nabla_u E_s-2A(\partial\mathbf{u}/\partial n)]=0 \quad (2)$$

where $\mathbf{u}=\mathbf{M}/M$ is a unit vector along the magnetization $\mathbf{M}$. The symbols E_v and E_s denote the volume and surface density, respectively, of the total energy other than ferromagnetic exchange. Each of the quantities γ, A, ∇_u, and $\partial/\partial n$ is defined in Ref. 2, and the coordinate system to be used is depicted in Fig. 1. The damping of

the magnetization is neglected, and it is assumed that the ferromagnetic film is sufficiently thin for skin-depth effects and electromagnetic propagation effects to be negligible.

By means of a straightforward calculation, we obtain from Eq. (1) the θ and ϕ component equations

$$-(M/\gamma)(\sin\theta)(\partial\theta/\partial t)+\partial E_v/\partial\phi -2A(\sin 2\theta)(\nabla\theta\cdot\nabla\phi)-2A(\sin^2\theta)\nabla^2\phi=0 , \quad (3)$$

$$(M/\gamma)(\sin\theta)(\partial\phi/\partial t)+\partial E_v/\partial\theta + A(\sin 2\theta)(\nabla\phi)^2-2A\nabla^2\theta=0 , \quad (4)$$

and from Eq. (2) the θ and ϕ component equations

$$\partial E_s/\partial\phi-2A(\sin^2\theta)(\partial\phi/\partial n)=0 , \quad (5)$$

$$\partial E_s/\partial\theta-2A(\partial\theta/\partial n)=0 . \quad (6)$$

We then introduce the decompositions

$$\theta=\theta_0+\theta_1 , \quad (7)$$

$$\phi=\phi_0+\phi_1 , \quad (8)$$

where the subscripts 0 and 1 denote the static and time-dependent components, respectively. After substitution of Eqs. (7) and (8) into Eqs. (3)–(6) we retain, at this point, only those terms which do not contain either θ_1 or ϕ_1. This leads to the static magnetization equations

$$(\partial E_v/\partial\phi)_0-2A(\sin 2\theta_0)(\nabla\theta_0\cdot\nabla\phi_0) -2A(\sin^2\theta_0)\nabla^2\phi_0=0 , \quad (9)$$

$$(\partial E_v/\partial\theta)_0+A(\sin 2\theta_0)(\nabla\phi_0)^2-2A\nabla^2\theta_0=0 , \quad (10)$$

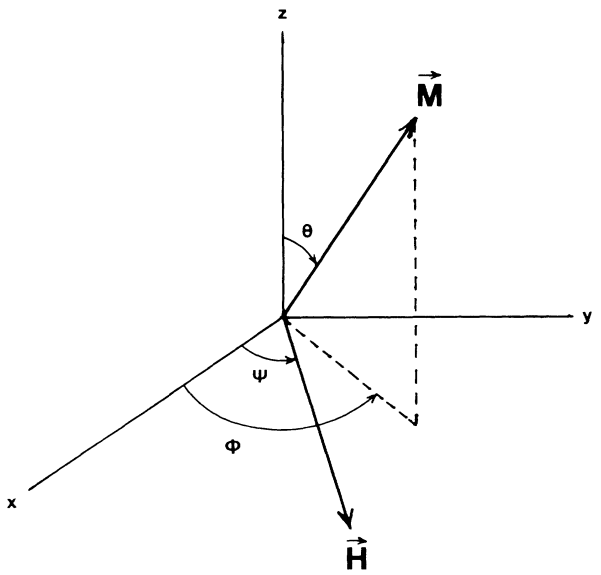

FIG. 1. Orientation of the Cartesian-coordinate system used in the calculations. The amorphous film is bounded by the planes $y=\pm L$ but unbounded along the x and z axes. The applied static magnetic field **H** and the instantaneous magnetization **M** are also shown.

and to the static boundary conditions

$$(\partial E_s/\partial\phi)_0-2A(\sin^2\theta_0)(\partial\phi_0/\partial n)=0 , \quad (11)$$

$$(\partial E_s/\partial\theta)_0-2A(\partial\theta_0/\partial n)=0 . \quad (12)$$

Next we seek those orientations of the static magnetization which are spatially uniform. These orientations are of particular interest because it is only for a spatially uniform static magnetization that the dynamic magnetization can be described relatively simply, namely by differential equations with constant coefficients. By inspection of Eqs. (9)–(12) we obtain

$$(\partial E_v/\partial\phi)_0=(\partial E_v/\partial\theta)_0=(\partial E_s/\partial\phi)_0=(\partial E_s/\partial\theta)_0=0 \quad (13)$$

as the necessary and sufficient condition for the static magnetization to be uniform.

Returning to the equations obtained upon substituting Eqs. (7) and (8) into Eqs. (3)–(6), we now retain only those terms which are of first order in θ_1 and ϕ_1. The resulting equations will not be presented explicitly because we immediately begin to simplify them by assuming the static magnetization orientations to be uniform. Thus we equate to zero all terms containing $\nabla\theta_0$, $\nabla\phi_0$, $\nabla^2\phi_0$, and $\partial\phi_0/\partial n$. This yields the dynamical magnetization equations

$$-(M/\gamma)(\sin\theta_0)(\partial\theta_1/\partial t)+(\partial^2E_v/\partial\theta\,\partial\phi)_0\theta_1 +(\partial^2E_v/\partial\phi^2)_0\phi_1-2A(\sin^2\theta_0)\nabla^2\phi_1=0 , \quad (14)$$

$$(M/\gamma)(\sin\theta_0)(\partial\phi_1/\partial t)+(\partial^2E_v/\partial\theta\,\partial\phi)_0\phi_1 +(\partial^2E_v/\partial\theta^2)_0\theta_1-2A\nabla^2\theta_1=0 , \quad (15)$$

and the dynamical boundary conditions

$$(\partial^2E_s/\partial\phi^2)_0\phi_1-2A(\sin^2\theta_0)(\partial\phi_1/\partial n) +(\partial^2E_s/\partial\theta\partial\phi)_0\theta_1=0 , \quad (16)$$

$$(\partial^2E_s/\partial\theta^2)_0\theta_1-2A(\partial\theta_1/\partial n)+(\partial^2E_s/\partial\theta\partial\phi)_0\phi_1=0 . \quad (17)$$

To show that the static magnetization is indeed uniform, as assumed in Eqs. (14)–(16), we must still use the necessary and sufficient condition which is embodied in Eq. (13) and thus depends on the expression chosen for E_v and E_s. Before doing that, however, we note that each of the quantities θ_1 and ϕ_1 will be assumed to be proportional to $\exp(i\omega t+ky)$, where ω is the circular frequency and k is the (as yet unknown) propagation constant. As shown below, k must be purely real, corresponding to surface waves, or purely imaginary, corresponding to spin waves.

Any significant progress beyond this point requires the use of Eq. (13) and hence the specification of explicit expressions for E_v and E_s. With a view toward the experiments of Ref. 1 we assume that E_v is given by

$$E_v=-MH(\cos\psi\sin\theta\cos\phi+\sin\psi\sin\theta\sin\phi +2\pi M^2\sin^2\theta\sin^2\phi) , \quad (18)$$

i.e., by the sum of a Zeeman term and a demagnetizing term. We neglect terms arising from crystalline volume anisotropy because the films under consideration are amorphous. If the method of film preparation gives rise to a deposition-induced volume anisotropy, then an additional term can easily be added to Eq. (18).

We assume that even near the film surface the magnetization is homogeneous. We further assume that E_s is given by

$$E_s = -K_s \sin^2\theta \sin^2\phi \ , \tag{19}$$

i.e., solely by the lowest-order term of the surface anisotropy energy density allowed by symmetry. According to Eq. (19) the y axis is the easy or hard axis of the surface anisotropy depending on whether K_s is positive or negative.[7] Since **H** is in the xy plane, as shown in Fig. 1, there is no reason for the spatially uniform static magnetization to have a component along the z axis. Thus we take the value of θ_0 to be $\pi/2$ and find that Eq. (13) yields the two solutions

$$\psi = 0 \ , \quad \theta_0 = \pi/2 \ , \quad \phi_0 = 0 \ , \tag{20}$$

$$\psi = \pi/2 \ , \quad \theta_0 = \pi/2 \ , \quad \phi_0 = \pi/2 \ , \tag{21}$$

which represent the only spatially uniform orientations of the static magnetization. It is just these experimental arrangements ($\psi = 0$ and $\pi/2$) which were used in Ref. 1.

B. Parallel FMR configuration

To treat the parallel FMR configuration we substitute Eqs. (18)–(20) into Eqs. (14)–(17). In this way we obtain the particularized form of the dynamical magnetization equations

$$(i\omega/\gamma)M\theta_1 - (MH + 4\pi M^2 - 2Ak^2)\phi_1 = 0 \ , \tag{22}$$

$$(MH - 2Ak^2)\theta_1 + (i\omega/\gamma)M\phi_1 = 0 \ , \tag{23}$$

and the particularized form of the dynamical boundary conditions

$$K_s\phi_1 + A\,\partial\phi_1/\partial n = 0 \ , \tag{24}$$

$$\partial\theta_1/\partial n = 0 \ . \tag{25}$$

In order that Eqs. (22) and (23) possess a nonvanishing solution, the secular determinant of their coefficients must vanish. This requirement yields the dispersion relation

$$\omega/\gamma = \{[H - (2Ak^2/M)][H + 4\pi M - (2Ak^2/M)]\}^{1/2} \ , \tag{26}$$

which is quadratic in k^2 and has the two pairs of roots

$$(2A/M)k_{1,2}^2 = H + 2\pi M - [(2\pi M)^2 + (\omega/\gamma)^2]^{1/2} \ , \tag{27}$$

$$(2A/M)k_{3,4}^2 = H + 2\pi M + [(2\pi M)^2 + (\omega/\gamma)^2]^{1/2} \ , \tag{28}$$

which correspond to two modes degenerate in energy. Since the frequency ω is a real number (because we continue to neglect damping), we see from Eqs. (27) and (28) that each of the quantities $k_{1,2}$ and $k_{3,4}$ must be purely real or purely imaginary. From Eq. (22) or Eq. (23) we obtain the amplitude ratio

$$v = \phi_1/\theta_1 = (i\gamma/\omega)[H - (2A/M)k^2] \ , \tag{29}$$

which may be combined with Eqs. (27) and (28) to give

$$v_{1,2} = (i\gamma/\omega)\{[(2\pi M)^2 + (\omega/\gamma)^2]^{1/2} - 2\pi M\} \ , \tag{30}$$

$$v_{3,4} = -(i\gamma/\omega)\{[(2\pi M)^2 + (\omega/\gamma)^2]^{1/2} + 2\pi M\} \ , \tag{31}$$

where v_n is the value of v for $k = k_n$. The modes corresponding to Eqs. (30) and (31), i.e., to Eqs. (27) and (28), represent an elliptical precession of the magnetization in the Larmor and anti-Larmor sense, respectively.

The general solutions of Eqs. (22) and (23) are

$$\theta_1 = C_1\cosh(k_1 y) + C_2\cosh(k_3 y) + C_3\sinh(k_1 y) + C_4\sinh(k_3 y) \ , \tag{32}$$

$$\phi_1 = C_1 v_1\cosh(k_1 y) + C_2 v_3\cosh(k_3 y) + C_3 v_1\sinh(k_1 y) + C_4 v_3\sinh(k_3 y) \ , \tag{33}$$

where C_1, C_2, C_3, and C_4 are unknown coefficients, k_1 and k_3 are the positive roots of Eqs. (27) and (28), respectively, and the factor $\exp(i\omega t)$ is suppressed. The expressions (32) and (33) must now be made to satisfy the boundary condition Eqs. (24) and (25) at each of the film surfaces $y = \pm L$. But if the boundary conditions are symmetric, as we assume in this paper, then they need be satisfied by only those parts of θ_1 and ϕ_1 which are symmetric. The secular equation arising from the boundary conditions has the solution

$$Ak_1k_3[1 - (v_3/v_1)]\sinh(k_1L)\sinh(k_3L) = K_s[k_3\sinh(k_3L)\cosh(k_1L) - (v_3/v_1)k_1\sinh(k_1L)\cosh(k_3L)] \ , \tag{34}$$

which may be used with the help of Eqs. (27) and (28) for calculating the desired resonance field $H = H_{\rm res}^{\parallel}$ corresponding to the parallel FMR configuration. Another form of Eq. (34) can be obtained in two special cases. In one of these cases k_1 and k_3 are purely real, and in the other case k_1 and k_3 are purely imaginary with $\cosh(k_1L) \neq 0$ and $\cosh(k_3L) \neq 0$. For either of these cases we can express Eq. (34) in the form

$$2A(1+\Delta)k_1k_3\tanh(k_1L)\tanh(k_3L) = K_3[(2+\Delta)k_1\tanh(k_1L) + (\Delta)k_3\tanh(k_3L)] \ , \tag{35}$$

where Δ is defined by

$$\Delta = [1 + (\omega/2\pi M\gamma)^2]^{1/2} - 1 \ . \tag{36}$$

It was the set of Eqs. (27), (28), (35), and (36) which we presented in Ref. 1 for the parallel FMR configuration without proof or discussion. In that reference we used Eqs. (27) and (28) to calculate $H_{\rm res}^{\parallel}$ from Eq. (34) rather than from the Eq. (35) presented there.

Turning now to the nature of the dynamic magnetization in the parallel FMR configuration, we begin by considering Eqs. (27) and (28). From Eq. (27) we see that $k_{1,2}^2$ may be positive or negative, depending on the magnitude of H. If $k_{1,2}^2$ is positive, then $k_{1,2}$ is real, which

corresponds to surface modes, but if $k_{1,2}^2$ is negative, then $k_{1,2}$ is imaginary, which corresponds to spin-wave modes. From Eq. (28), on the other hand, it follows that $k_{3,4}^2$ is always positive so that $k_{3,4}$ is always real and corresponds to surface modes. To determine whether $k_{1,2}$ is real or imaginary we must consider Eq. (34). The quantity v_3/v_1 appearing in this equation is always negative, as shown by Eqs. (30) and (31). Thus Eq. (34) shows that if K_s is positive then the mode corresponding to k_1 is either a (unique) surface mode or some (nonunique) spin-wave mode. If, however, K_s is negative then k_1 can correspond to a (nonunique) spin-wave mode only. We emphasize, at this point, that if K_s is not zero then the k_1 and k_3 modes are both needed to satisfy the boundary conditions. If K_s vanishes then only the k_1 mode can exist.

C. Perpendicular FMR configuration

The treatment of the perpendicular FMR configuration involves substitution of Eqs. (18), (19), and (21) into Eqs. (14)–(17). This leads to the particularized form of the dynamical equations,

$$(i\omega/\gamma)M\theta_1-(MH-4\pi M^2-2Ak^2)\phi_1=0 , \quad (37)$$

$$(MH-4\pi M^2-2Ak^2)\theta_1+(i\omega/\gamma)M\phi_1=0 , \quad (38)$$

and the particularized form of the dynamical boundary conditions,

$$K_s\phi_1-A\,\partial\phi_1/\partial n=0 , \quad (39)$$

$$K_s\theta_1-A\,\partial\theta_1/\partial n=0 . \quad (40)$$

The requirement that Eqs. (46) and (47) possess a nonvanishing solution yields the dispersion relation

$$\omega/\gamma=H-4\pi M-2Ak^2/M . \quad (41)$$

Since ω is a real number (because we continue to neglect damping), Eq. (41) shows that k must be purely real or purely imaginary. From Eq. (37) or (38) we obtain the amplitude ratio

$$v=\phi_1/\theta_1=(i\gamma/\omega)(H-4\pi M-2Ak^2/M) , \quad (42)$$

which may be combined with Eq. (41) to give

$$v=i . \quad (43)$$

Thus the precession of the magnetization is circular and there are no degenerate modes.

The general solutions of Eqs. (37) and (38) are

$$\theta_1=D_1\cosh(ky)+D_2\sinh(ky) , \quad (44)$$

$$\phi_1=D_1v\cosh(ky)+D_2v\sinh(ky) , \quad (45)$$

which are analogous to Eqs. (32) and (33). Here D_1 and D_2 are unknown coefficients and the factor $\exp(i\omega t)$ is suppressed. The expressions (44) and (45), of course, must be made to satisfy the boundary conditions (39) and (40) at each of the film surfaces $y=\pm L$. For reasons explained just after Eq. (33), however, the boundary conditions need be satisfied by only the symmetric parts of θ_1 and ϕ_1. This requirement leads to

$$Ak\tanh(kL)=-K_s , \quad (46)$$

which may be used in conjunction with Eq. (41) for calculating the desired resonance field $H=H_{\rm res}^{\perp}$. It was the Eqs. (41) and (42) which we presented in Ref. 1 for the perpendicular FMR configuration without proof or discussion.

The nature of the dynamic magnetization in the perpendicular FMR configuration can be discussed by a method analogous to that used for the parallel FMR configuration. We find, on the basis of Eq. (46), that if K_s is positive then k can only correspond to a (unique) spin-wave mode, and that if K_s is negative then k can correspond either to a (unique) surface mode or to a (nonunique) spin-wave mode.

III. DETERMINATION OF THE SURFACE ANISOTROPY

In this section we use the theory of Sec. II and the experimental FMR data of Ref. 1 to determine the surface anisotropy constant K_s of amorphous films of Fe_xB_{100-x}. Since the preparation of the films and the method of measurement have already been discussed in Ref. 1, we now turn directly to the experimental and theoretical results. For the $x=50$ films the data corresponding to the parallel FMR configuration were taken at 9.52 and 24.03 GHz, and the data corresponding to the perpendicular configuration were taken at 9.52 GHz. The experimental points and theoretical lines for the parallel configuration are shown in the upper part of Fig. 2 and for the perpendicular configuration in the lower part of Fig. 2. We note that both experimentally and theoretically the sign of the slope of $H_{\rm res}$ versus $1/(2L)$ is opposite in the two configurations. For the $x=70$ films the parallel configuration only was used for both the 9.52- and 24.03-GHz data, and the corresponding experimental points and theoretical curves are shown in Fig. 3.

Since the thicknesses $2L$ of our Fe_xB_{100-x} films are known from direct measurements, we may calculate $H_{\rm res}^{\parallel}$ as a function of $1/L$ by substituting Eqs. (27) and (28) into Eq. (34). Such a calculation clearly requires that all the other quantities appearing in these equations be known. Actually, however, the values of K_s are unknown and the values of M are known for bulk samples only. Although the parameters g and A are not well known, we can approximate g by the value 2.09 appropriate for metallic iron, and A by the values 5.5×10^{-7} erg/cm for $x=50$ and 1.38×10^{-6} erg/cm for $x=70$ derived in the Appendix from published values of the Curie temperature.

To determine the values of K_s and M for a given x we fitted suitable theoretical curves of $H_{\rm res}^{\parallel}$ versus $1/L$ to the experimental points shown in Fig. 2. Specifically, we began by assuming a reasonable value for M and then calculating K_s from Eq. (34). For $x=50$, for example, we used the initial value $M=450$ emu previously measured[8] for $x=48$. In this way we calculated a K_s value corresponding to each of the six L values. Next we varied the initial M value in steps of 10 emu until we at-

tained that final M for which the root-mean-square deviation of the six calculated K_s values from their average became a minimum. The average K_s value corresponding to this minimum root-mean-square deviation was then adopted together with the final M value as being the "best-fit values" of K_s and M. These latter values, namely $K_s = 0.20$ erg/cm^2 and $M = 570$ emu, were then used for calculating $H^{\parallel}_{\rm res}$ as a function of $1/L$ from Eqs. (27), (28), and (34). For the $x = 70$ films we started with the value $M = 1300$ emu previously measured[8] for $x = 71$. We thus obtained the best-fit values $K_s = 0.53$ erg/cm^2 and $M = 1240$ emu, which we then used in Eqs. (27), (28), and (34) to calculate $H^{\parallel}_{\rm res}$ as a function of $1/L$. For the perpendicular FMR configuration these same best-fit values of K_s and M for $x = 50$ were then substituted into Eqs. (41) and (46) in order to calculate the $1/L$ dependence of $H^{\perp}_{\rm res}$.

Figures 2 and 3 show that in almost all cases the agreement between theory and experiment is quite good at both frequencies and both FMR configurations. The best-fit values of K_s and M are seen to predict 16 of the 18 experimental values of $H_{\rm res}$ in the case of $x = 50$ and all 10 experimental values of $H_{\rm res}$ in the case of $x = 70$. For $x = 50$ the $H^{\perp}_{\rm res}$ values of the two thinnest films do show some discrepancy between theory and experiment. This is easily understood, however, because in those cases $H^{\perp}_{\rm res}$ is smaller than $4\pi M$ so that the films are not saturated sufficiently. It should also be noted that the generally good agreement between theory and experiment does not seem to be invalidated by uncertainties in the values of A. This is shown most clearly by the fact that a change of as much as a factor of 2 in the value of A gives rise to deviations of less than 3% in the best-fit values of K_s and M.

Next we offer some comments on the K_s values and M values determined in this paper. We note, first of all, that for a given x the experimental values of $H^{\parallel}_{\rm res}$ shown in Figs. 2 and 3 are larger than the value of H calculated from Eq. (26) for $k = 0$, i.e., for the uniform mode. This means, according to Eq. (27), that $k^2_{1,2}$ is positive. Thus

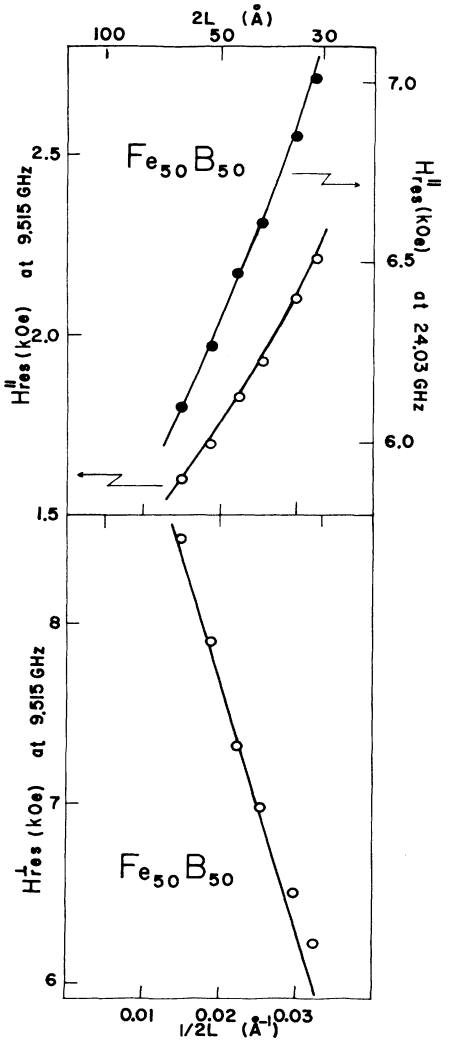

FIG. 2. FMR in $Fe_{50}B_{50}$: Experiment (data points) and theory (lines based on the best-fit values $K_S = 0.20$ erg/cm^2 and $M = 570$ emu, and on the estimated values $A = 5.5 \times 10^{-7}$ erg/cm and $g = 2.09$).

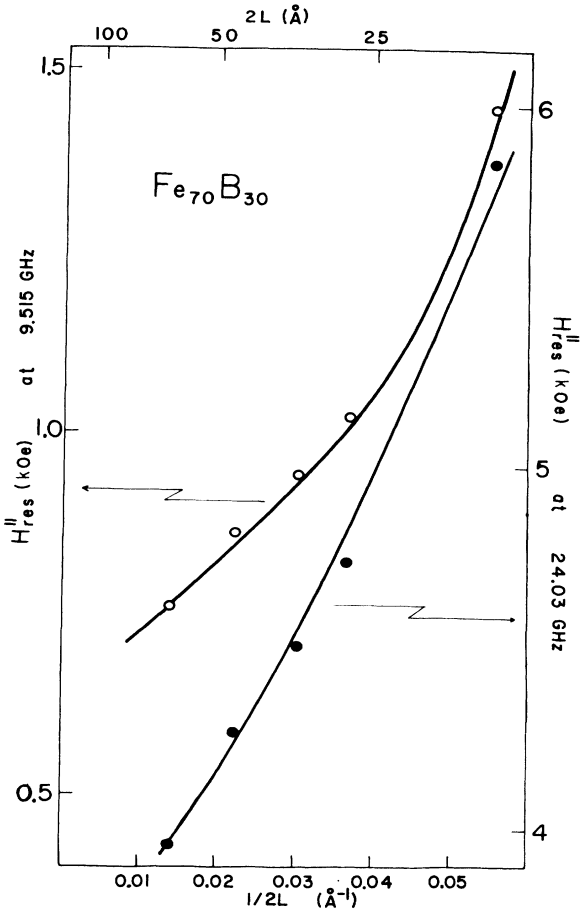

FIG. 3. FMR in $Fe_{70}B_{30}$: Experiment (data points) and theory (lines based on the best fit values $K_s = 0.53$ erg/cm^2 and $M = 1240$ emu, and on the estimated values $A = 1.38 \times 10^{-6}$ erg/cm and $g = 2.09$).

$k_{1,2}$ is real so that our definition [see the text following Eq. (33)] requires k_1 to be positive. Since Eq. (28) shows that $k_{3,4}^2$ is always positive, $k_{3,4}$ is necessarily real and, hence, k_3 is positive. Equation (34) shows, therefore, that in our experiments involving $H_{\rm res}^{\parallel}$ the value of K_s must be positive, in agreement with the results of the curve-fitting procedure described above. Analogous considerations based on Eqs. (41) and (46) show that our experimental values of $H_{\rm res}^{\perp}$ require K_s to be positive in the perpendicular FMR configuration also.

Secondly, we note that the use of two adjustable parameters (namely K_s and M) in our curve-fitting procedure may conceivably cause the agreement between theory and experiment to be accidental, especially since the value of M may well be L dependent. To investigate this possibility we used SQUID magnetometry to measure[9] directly the M values of the films used in the FMR work. We found that these values are essentially independent of L and that they confirm adequately the M values obtained by fitting theoretical curves to experimental FMR data. Accordingly, we used the directly measured M values for calculating K_s, the only adjustable parameter in this case. By requiring this K_s to fit, within the $\pm 10\%$ experimental error in $2L$, all the experimental data for the ultrathin films used in the FMR experiments, we estimated that the error associated with the values $K_s = 0.20$ and 0.53 erg/cm^2 determined above is ± 0.06 and ± 0.16 erg/cm^2, respectively. Thus the results of the direct measurements of M provide substantial support for the reliability of the FMR method presented in this paper for determinations of K_s and M.

APPENDIX

In this Appendix we estimate the values of the exchange stiffness constant A for Fe_xB_{100-x} by using published values of the Curie temperature T_C. Directly measured values of A do not seem to be available for these alloys.

We begin with the approximate empirical expression[10]

$$k_B T_C / J = \tfrac{5}{96}(z-1)[11S(S+1)-1] , \tag{A1}$$

which relates T_C to the exchange integral J. Here k_B is Boltzmann's constant, S is the spin per magnetic atom, and z is the number of nearest neighbors of a magnetic atom. To relate J to A we use the equation[11]

$$A = \tfrac{1}{6} J N z S^2 r^2 , \tag{A2}$$

where r is the most probable distance between nearest-neighbor magnetic atoms and N is the total number of atoms per unit volume. By combining Eqs. (A1) and (A2) we obtain

$$A = \frac{\frac{16}{5} k_B T_C N z S^2 r^2}{(z-1)[11S(S+1)-1]} \tag{A3}$$

as the desired relation between A and T_C. To find the value of z we adopt the dense random-packing model[12] and use the binomial distribution function

$$P(z) = \frac{c!}{z!(c-z)!} \left[\frac{x}{100} \right]^z \left[1 - \frac{x}{100} \right]^{c-z} , \tag{A4}$$

which gives the probability of finding z neighboring Fe atoms ($z = 0, 1, 2, \ldots, c$) in amorphous Fe_xB_{100-x} having the coordination number c. Next we assume[13] the value $c = 12$ and determine z by maximizing $P(z)$ with respect to z. In this way we obtain $z = 6$ for $x = 50$ and $z = 9$ for $x = 70$.

For the value of N of Fe_xB_{100-x} we use

$$N = \frac{(100) d_x N_0}{x A_{\rm Fe} + (100-x) A_{\rm B}} , \tag{A5}$$

where N_0 is Avogadro's number, $A_{\rm Fe}$ and $A_{\rm B}$ are the atomic masses of Fe and B, respectively, and d_x is the density. The latter may be approximated by

$$d_x = \frac{[x A_{\rm Fe} + (100-x) A_{\rm B}] d_{\rm Fe} d_{\rm B}}{x A_{\rm Fe} d_{\rm B} + (100-x) A_{\rm B} d_{\rm Fe}} , \tag{A6}$$

where $d_{\rm Fe}$ and $d_{\rm B}$ denote, respectively, the density of Fe and B. For the estimates which follow we use the tabulated values $A_{\rm Fe} = 55.86$, $A_{\rm B} = 5$, $d_{\rm Fe} = 7.86$ g/cm^3, and $d_{\rm B} = 2.34$ g/cm^3, as well as the rough estimate $r = 2.6 \times 10^{-8}$ cm (based on the crystalline counterpart of $Fe_{70}B_{30}$) which we used for $Fe_{50}B_{50}$ as well as for $Fe_{70}B_{30}$. In addition, we use several values inferred from experiments, namely $S = \frac{1}{2}$ (Ref. 14) and $T_C = 530$ K (Ref. 15) for $x = 50$ and $S = 1$ (Ref. 13), and $T_C = 750$ K (Ref. 15) for $x = 70$. On this basis Eq. (A3) yields $A = 55 \times 10^{-7}$ and 1.38×10^{-6} erg/cm for $x = 50$ and 70, respectively. These estimates of A clearly involve several assumptions, and for an arbitrary material a better method of estimating A may well be developed. It is fortunate, therefore, that $H_{\rm res}$ does not depend on A very sensitively, as shown quantitatively in Sec. III.

---

[1] L. Zhang, G. T. Rado, S. H. Liou, and C. L. Chien, J. Magn. Magn. Mater. **54-57**, 765 (1986). This paper contains the following three misprints: On p. 765, left-hand column, in the seventh line from the bottom, 100 should be replaced by 170, and in the sixth line from the bottom, 170 should be replaced by 100; on p. 766, in the equation for $H_{\rm res}$, the term $-2M$ should be replaced by $-2\pi M$. It should also be noted that for the final measurements of $H_{\rm res}$ the amorphous film samples were mounted on the wide sidewall of the rectangular cavity rather than on the Teflon rod used for $H_{\rm res}$. In this way, the sample alignment was made more accurate and effects due to vibrations of the Teflon rod were minimized.

[2] G. T. Rado, Phys. Rev. B **26**, 295 (1982); **32**, 6061(E) (1985).

[3] H. Puszkarski, Prog. Surf. Sci. **9**, 191 (1979).

[4] U. Gradmann, J. Magn. Magn. Mater. **54-57**, 733 (1986).

[5] L. Landau and E. Lifshitz, Phys. Z. Sowjetunion **8**, 153 (1935).

[6] G. T. Rado and J. R. Weertman, J. Phys. Chem. Solids **11**, 315 (1959).

[7]G. T. Rado and L. Zhang, Phys. Rev. B **33**, 5080 (1986), discuss the signs of surface anisotropy constants in *monocrystals.*
[8]F. Stobiecki, J. Magn. Magn. Mater. **41**, 195 (1984).
[9]L. Zhang and G. T. Rado, J. Appl. Phys. **61**, 4265 (1987).
[10]G. S. Rushbrooke and P. J. Wood, Mol. Phys. **1**, 257 (1958).
[11]A. Gangulee and R. J. Kobliska, J. Appl. Phys. **49**, 4896 (1978).
[12]J. F. Sadoc, J. Dirmier, and A. Guinier, J. Non-Cryst. Solids **12**, 46 (1973).
[13]C. L. Chien, D. Musser, E. M. Gyorgy, R. C. Sherwood, and H. S. Chen, Phys. Rev. B **20**, 283 (1979).
[14]D. J. Webb and S. M. Bhagat, IEEE Trans. Magn. **MAG-19**, 1892 (1983).
[15]C. L. Chien and K. M. Unruh, Phys. Rev. B **24**, 1556 (1981); **25**, 5790 (1982); **29**, 207 (1984).